Mechanical Systems and Signal Processing 85 (2017) 857–866

Contents lists available at ScienceDirect

Mechanical Systems and Signal Processing

journal homepage: www.elsevier.com/locate/ymssp

Tooth modification and dynamic performance of the cycloidal drive

Zhong-Yi Ren[a,b,*], Shi-Min Mao[a], Wen-Chao Guo[a], Zheng Guo[a]

[a] State Key Laboratory for Manufacturing System Engineering, Xi'an Jiaotong University, Xi'an 710049, China
[b] School of Mechanical Engineering of NingXia University, NingXia 750021, China

ARTICLE INFO

Keywords:
Cycloidal drive
Tooth modification
Runge-kutta numerical method

ABSTRACT

A new method of cycloid disc tooth modification is presented in this paper. Its main idea is to design the modification clearance curves to adapt to different modification targets. A detailed procedure of the new modification clearance curve, which can be defined by adjusting the position of 5 key points is developed. Numerical experiments are carried out to verify the effectiveness of the new method. A Multi-DOF nonlinear dynamic model of cycloidal speed reducer is established, then the cycloid disc rotational displacement and rotational velocity versus time of different modification clearance are solved by the Runge-kutta numerical method. The results show that this method can improve the carrying capability of cycloidal drive, eliminate noise and vibration and develop the transmission accuracy.

1. Introduction

Cycloidal speed reducers are widely used due to their excellent characteristics, such as compact structure, long work life, high torque ratio, extremely reliable functioning in dynamical load conditions, and high efficiency coefficient. The general applications of cycloidal speed reducers are in robot industry, satellite technology, elevators, the process industry, transporters, etc.

The basic methods of profile generation of cycloid disc teeth are given in Refs. [1–5]. Litvin and Feng [6] developed a general method for the generation and design of cycloid disc teeth profile. Hsieh [7] studied the epitrochoidal and hypotrochoidal profiles based on the theory of gearing. Sensinger [8] presented an unified approach to cycloidal drive profile, stress and efficiency optimization with closed-form equations. Blanche and Yang [9,10] analyzed the effects of machining tolerances on backlash and torque ripples. Yongkuan [11] analyzed a mathematical model for the geometric lost motion of high accurate RV reducer used in robot. Huang [12] studied the profile modification and tooth contact analysis of the cycloidal drive. In order to improve the working performance, such as the distribution of the forces, stress and deformations of cycloid discs, a profile modification method of cycloid disc teeth is discussed in Ref. [13]. Chmurawa and John [14] analyzed the forces, stress and strain of cycloid disc with a modified profile by using a finite elements method. Yunhong et al. [15] derived a mathematical model of 2K-H pin cycloid planetary mechanism under the influence of friction. Hwang and Hsieh [16] determined a feasible design region without undercutting on the teeth profile or interference between the adjacent pins. The dynamic behavior of a cycloidal speed reducer is presented in Refs. [17–19]. Han Linshan discussed the dynamic transmission accuracy of the RV reducer [20,21].

A new method of cycloid disc tooth modification is presented in this paper. A Multi-DOF nonlinear dynamic model of cycloidal speed reducer is established, and the cycloid disc rotational displacement and rotational velocity versus time of different modification clearance are gained, through the Runge-kutta numerical method.

* Corresponding author at: State Key Laboratory for Manufacturing System Engineering, Xi'an Jiaotong University, Xi'an 710049, China.
E-mail address: rzy025@sina.com (Z.-Y. Ren).

http://dx.doi.org/10.1016/j.ymssp.2016.09.029
Received 30 June 2016; Received in revised form 7 September 2016; Accepted 17 September 2016

2. Principle of cycloidal drive and tooth modification method of cycloid disc today

An exploded view of a one-stage cycloidal drive is shown in Fig. 1(A). The working principle is as follows. Crank shaft (2) rotates with the input shaft (1), and cycloid discs (3) are connected with the crank shaft (2). Cycloid discs which are installed in the ring gear (5) are conjugated with the cylinder called pin (4). Output rollers (6) which go through the circular openings of the cycloid discs and transfer their motion to the output shaft are tightly connected to the output shaft (7).

The cycloid disc teeth profile can be expressed as [22]:

$$\begin{cases} x_c = [r_p - r_{rp}\phi^{-1}(K_1, \varphi)] \times \cos[(1 - i^H)\varphi] - [a - K_1 r_{rp}\phi^{-1}(K_1, \varphi)] \times \cos(i^H\varphi) \\ y_c = [r_p - r_{rp}\phi^{-1}(K_1, \varphi)] \times \sin[(1 - i^H)\varphi] + [a - K_1 r_{rp}\phi^{-1}(K_1, \varphi)] \times \sin(i^H\varphi) \end{cases} \quad (1)$$

where

$$\phi^{-1}(K_1, \varphi) = (1 + K_1^2 - 2K_1\cos\varphi)^{-1/2} \quad (2)$$

$$K_1 = az_p/r_p \quad (3)$$

$$i^H = z_p/z_c \quad (4)$$

where, r_p is the pin position (distance from pin center to O_p), as show in Fig. 1(B). r_{rp} is the radius of the pin. a is the eccentric distance. z_p is the number of pins.z_c is the number of teeth of cycloid disc. φ is the angle value of the pin position vector to O_cO_p. i^H is the transmission ratio.

Cycloidal drive has high contact ratio, nearly 50% of the cycloid disc teeth are meshing with pins simultaneously in theory. But in practice, in order to compensate the error of manufacture and installation, and maintain reasonable clearance for lubrication and ensure convenient installation and disassembly, it is necessary to modify the cycloidal disc profile.

There are three main kinds of cycloid disc teeth modification methods [23]:

Case a. Modification by pin radius r_{rp}.

In this type of modification, the result can be obtained by adding a small quantity of Δr_{rp} to r_{rp} in the profile Eq. (1).

Case b. Modification by pin positionr_p.

In this type of modification, the result can be obtained by adding a small quantity of Δr_p to r_p in the profile Eq. (1).

Case c. Compound modifications by r_{rp} and r_p.

In this type of modification, a small values of pin radius, Δr_{rp}, and pin position, Δr_p, will both be added to Eq. (1).

In case of teeth profile modification, generally only one contact line will remain, where the clearance is zero. Fig. 2 shows the modification clearance curve acquired by **case c**. The modification clearance curve is the clearance between the theoretical tooth profile and the modified tooth profile..

The cycloidal drive parameters used in this paper are shown in Table 1.

The contact stress of modified tooth profile and theoretical tooth profile are shown in Fig. 3, and the contact force of modified tooth profile and theoretical tooth profile are shown in Fig. 4.

As can be seen from Figs. 3 and 4, the contact stress and the contact force of cycloid drive are significantly increased by the

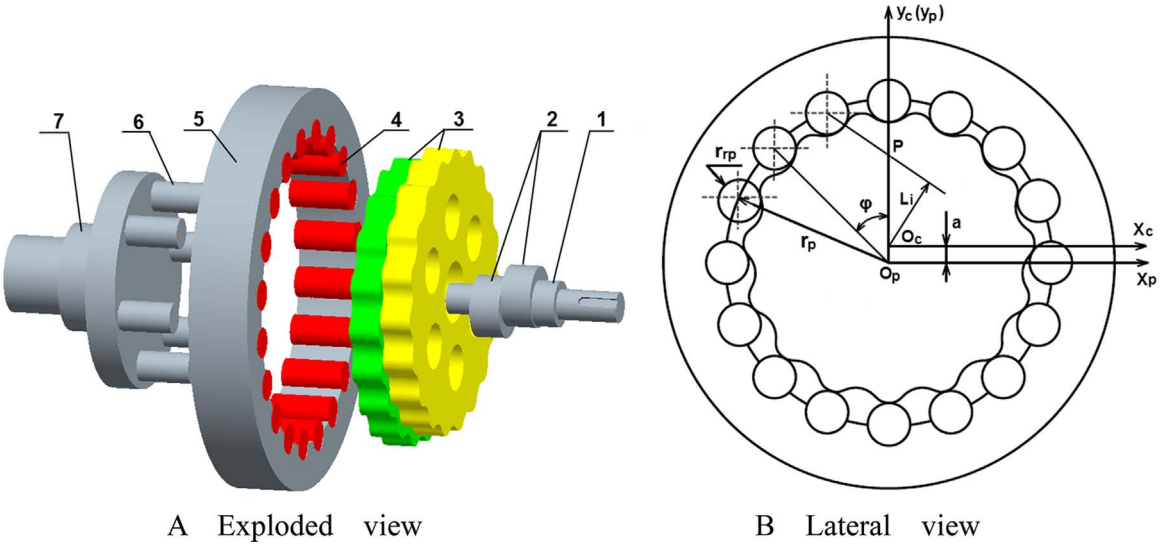

Fig. 1. One-stage cycloid gear reducer.

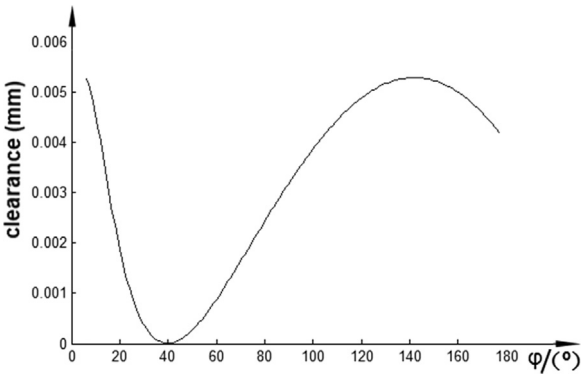

Fig. 2. Modification clearance curve.

Table 1
parameters of cycloidal drive.

Parameters	Value
Pin center circle radius (mm)	114.5
Pin radius (mm)	5
Eccentric distance (mm)	2.2
Pin number	40
Cycloid disc teeth number	39
Width of cycloid disc (mm)	18
Torque (N m)	2000
Elasticity modulus (M Pa)	2.06×10^5
Poisson's ratio	0.3
Modification parameter Δr_{rp} (mm)	−0.026
Modification parameter Δr_p (mm)	−0.3

current teeth profile modification methods. A new method of cycloid disc tooth modification is presented in this paper to improve the transmission performance of cycloid drive, such as carry capability, transmission accuracy, backlash, etc.

3. New modification method of cycloid disc and examples

3.1. New modification method

The small values of pin radius, Δr_{rp}, and pin position, Δr_p, introduced in **Section 2** are fixed. If they are variable along teeth profile, any modified tooth profile can be obtained by adding those variables to cycloid disc tooth profile equation. In this paper, the variable, Δr, which is a small variation of pin radius is introduced. The value of Δr along tooth profile and its approximate modification clearance curve are considered equal in this paper. The main idea of this new modification method presented in this paper is to design the modification clearance curve, i.e., design the value of Δr along tooth profile, and correct the modification clearance curve according to the modification target. The initial modification clearance curve designed in this paper is show in Fig. 5B. The modification clearance curve is divided into four sections by 5 key points according to its complication. Fig. 5A shows the location of 5 key points in the tooth profile, and Fig. 5B shows the location of 5 key points in the modification clearance curve.

As show in Fig. 5, the 5 key points are shown as.

$A(\varphi_A, \Delta r_A), B(\varphi_B, \Delta r_B), C(\varphi_C, \Delta r_C), D(\varphi_D, \Delta r_D), E(\varphi_E, \Delta r_E)$.

The four sections of clearance curve are.

$\widetilde{AB}, \widetilde{BC}, \widetilde{CD}$ and $\widetilde{DE}$.

where the points $A(\varphi_A, \Delta r_A)$ and $E(\varphi_E, \Delta r_E)$ are in the heel and toe end of the tooth.

Section $\widetilde{AB}$ and $\widetilde{DE}$ can be expressed as :

$$\Delta r = a_1\varphi^2 + b_1\varphi + c_1 \tag{5}$$

Section $\widetilde{BC}$ and $\widetilde{CD}$ can be expressed as:

$$\Delta r = a_2\varphi^3 + b_2\varphi^2 + c_2\varphi + d \tag{6}$$

$B(\varphi_B, \Delta r_B), C(\varphi_C, \Delta r_C), D(\varphi_D, \Delta r_D)$ are the extreme points, with

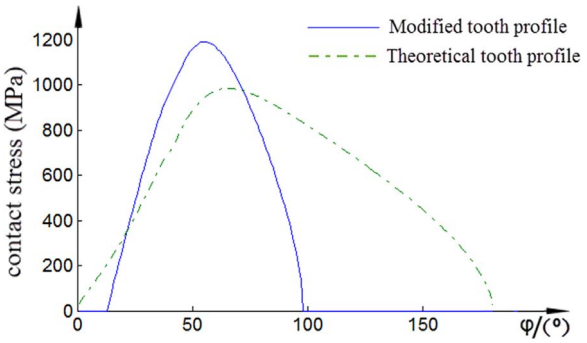

Fig. 3. Contact stress.

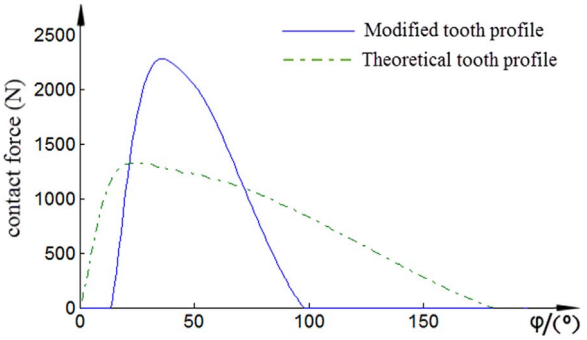

Fig. 4. Contact force.

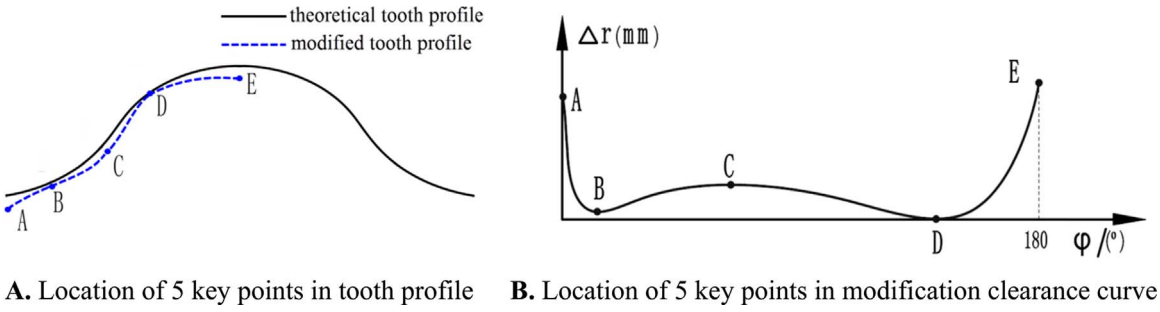

Fig. 5. Location of 5 key points.

$$\left.\frac{d\Delta r}{d\varphi}\right|_{B,C,D} = 0 \tag{7}$$

where, the coefficients a_1, b_1, c_1, a_2, b_2, c_2, d can be calculated by the coordinate values of 5 key points and Eq. (7).

In conclusion, the modification clearance curve can be obtained by the coordinate values of 5 key points. The key point of this new modification method presented in this paper is to calculate the coordinate values of these 5 key points. In order to achieve the modification target, the coordinate value of these 5 key points can be calculated as follows:

1. Point $A(\varphi_A, \Delta r_A)$ is located in the heel of the gear tooth, and point $E(\varphi_E, \Delta r_E)$ is located in the toe end of the gear tooth, so $\varphi_A = 0°, \varphi_E = 180°$.

   Since the modified cycloid disc teeth profile at section $\widetilde{AB}$ and section $\widetilde{DE}$ are not transmitting torque, the value of Δr_A, Δr_E, φ_B and φ_D can be selected according to the applications by designer. This is the advantage of this new modification method.
2. The other parameters such as Δr_B, Δr_C, Δr_D and φ_C need computer programming. The special programming process is shown as the following steps

   Step 1 Define the initial values of Δr_B, Δr_C, Δr_D, φ_C.
   Step 2 Calculate the gear tooth contact deformation.

$$w_i = \beta L_i - \Delta r_i. \tag{8}$$

where w_i is the contact deformation of the i-th pin and cycloid disc tooth. β is the cycloid disc rotate angle caused by elastic deformation, which needs to be given an initialized value. L_i is the moment arm of the i-th pin.

Step 3 Calculate the contact force according to the contact deformation.

Cylindrical and cylindrical contact deformation can be expressed as [22]:

$$w = \frac{2F}{\pi L}\left[\frac{1-\mu_1^{\ 2}}{E_1}\left(\frac{1}{3} + \ln\frac{4R_1}{b}\right) + \frac{1-\mu_2^{\ 2}}{E_2}\left(\frac{1}{3} + \ln\frac{4R_2}{b}\right)\right] \tag{9}$$

$$b = 1.6\sqrt{\frac{F}{L}K_D\left(\frac{1-\mu_1^{\ 2}}{E_1} + \frac{1-\mu_2^{\ 2}}{E_2}\right)} \tag{10}$$

$$K_D = \frac{2R_1R_2}{R_1 \pm R_2} \tag{11}$$

where, '+' is for-convex section of disc's tooth profile, and'−' is for concave section,$F$is the contact force (N), E_i is elasticity modulus (MPa), μ_i is the poisson's ratio, R_i is the radius of the two contact surface (mm) $i = 1, 2$.
L is the width of the effective tooth surface.

Step 4 Analyze the output torque according to contact force. If the output torque is not equal to rated output torque, correct the value of β and turn to step 2, else go to step 5.

Step 5 Calculate the modification target (such as contact stress, contact force). If it is not the optimal, correct the value of Δr_B, Δr_C, Δr_D,φ_C, and turn to step 2, else export the coordinate value of 5 key points.

The modification clearance curve can be obtained based on Eqs. (5)–(7) and the coordinate value of 5 key points. Adding Δr to r_{rp} in the profile Eq. (1), the modified cycloid disc teeth profile, i.e., the corresponding forming cutting tool profile can be expressed as:

$$\begin{cases} x_c = [r_p - (r_{rp} + \Delta r)\phi^{-1}(K_1, \varphi)] \times \cos[(1 - i^H)\varphi] \quad - [a - K_1(r_{rp} + \Delta r)\phi^{-1}(k_1, \varphi)] \times \cos(i^H\varphi) \\ y_c = [r_p - (r_{rp} + \Delta r)\phi^{-1}(K_1, \varphi)] \times \sin[(1 - i^H)\varphi] \quad + [a - K_1(r_{rp} + \Delta r)\phi^{-1}(k_1, \varphi)] \times \sin(i^H\varphi) \end{cases} \tag{12}$$

3.2. Modification examples

The cycloidal drive parameters used in this paper are shown in Table 1.

The modification targets generally consist of contact stress, contact force, transmission error, etc. If the modification target is contact stress, the 5 key points can be solved by computer program and be shown as:
$A(0, 0.02)$,$B(9, -0.0018)$,$C(54, 0.002)$,$D(160, 0)$,$E(180, 0.02)$

The clearance curve can be expressed as Eq. (13):

$$\begin{cases} \Delta r = 2.6914 \times 10^{-4}(\varphi - 9)^2 - 0.0018 & 0 \le \varphi < 9 \\ \Delta r = -7.32 \times 10^{-8}\varphi^3 + 7.137 \times 10^{-6}\varphi^2 - 1.107 \times 10^{-4}\varphi - 0.0013 & 9 \le \varphi < 54 \\ \Delta r = 3.556 \times 10^{-9}\varphi^3 - 1.152 \times 10^{-6}\varphi^2 + 9.558 \times 10^{-5}\varphi - 3.64 \times 10^{-4} & 54 \le \varphi < 160 \\ \Delta r = 3.8562 \times 10^{-5}(\varphi - 160)^2 & 160 \le \varphi < 180 \end{cases} \tag{13}$$

The clearance curve is shown in Fig. 6, and contact stress is shown in Fig. 7.

If the modification target is contact force, The 5 key points can be shown as:
$A(0, 0.02)$,$B(5, 0.002)$,$C(36, 0.0025)$,$D(150, 0)$,$E(180, 0.02)$

The clearance curve can be expressed as Eq. (14):

$$\begin{cases} \Delta r = 7.2 \times 10^{-4}(\varphi - 5)^2 + 0.002 & 0 \le \varphi < 5 \\ \Delta r = -4.1 \times 10^{-8}\varphi^3 + 2.398 \times 10^{-6}\varphi^2 - 2.09 \times 10^{-5}\varphi + 0.002 & 5 \le \varphi < 34 \\ \Delta r = 3.2 \times 10^{-9}\varphi^3 - 8.84 \times 10^{-7}\varphi^2 + 4.9 \times 10^{-5}\varphi + 0.0017 & 34 \le \varphi < 150 \\ \Delta r = 1.5022 \times 10^{-5}(\varphi - 150)^2 & 150 \le \varphi < 180 \end{cases} \tag{14}$$

The clearance curve is shown in Fig. 8, and contact force is shown in Fig. 9.

As can be seen from Figs. 7 and 9, the contact stress and the contact force can be significantly reduced by teeth profile modification.

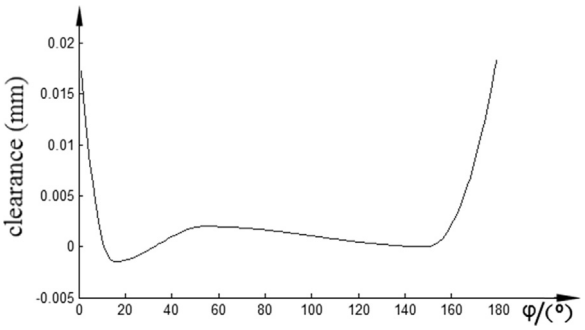

Fig. 6. Modification clearance.

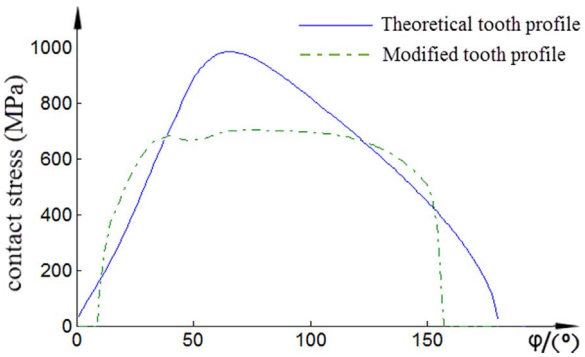

Fig. 7. Contact stress.

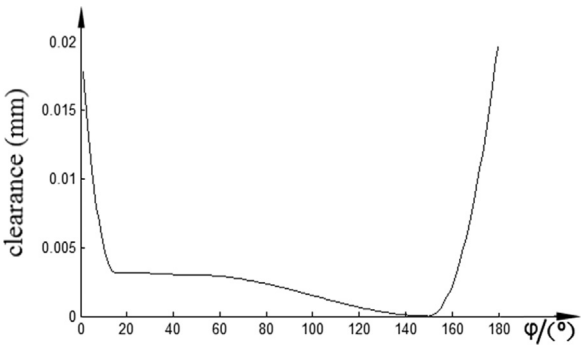

Fig. 8. Modification clearance.

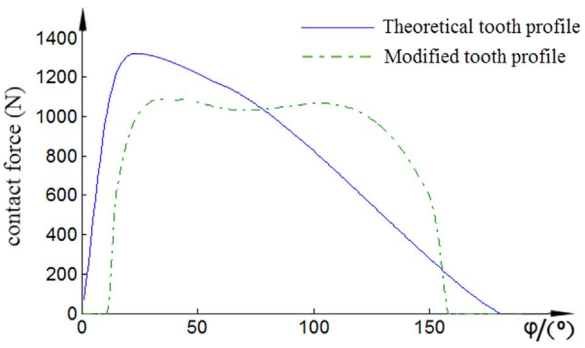

Fig. 9. Contact force.

4. The relationship between cycloid disc teeth profile modification and the dynamic performance of cycloidal speed reducer

Cycloid disc teeth profile modification will affect the dynamic performance of cycloidal speed reducer. In this paper, A five degree-of-freedom discrete dynamic model of cycloidal speed reducer is established as shown in Fig. 10.

As illustrated in Fig. 10, input shaft and crank shaft are fixed together. Each component is represented by a rigid disc of radius R and polar mass moment of inertia J. The cycloid disc mesh are represented by two sets of periodically time-varying mesh spring-damping elements with $K_m(t)$ and $C_m(t)$.

The crank shaft torsion is represented by two sets of spring-damping elements with K_a and C_a. The crank shaft and cycloid disc mesh is represented by two sets of spring-damping elements with K_h and C_h. The cycloid disc and output rollers mesh is represented by two sets of spring-damping elements with K_q and C_q.

With the positive directions of the alternating rotational displacements θ_a, θ_l, θ_m, θ_o and the constant external torques T_a and T_o are defined in Fig. 10, the equations of motion of the cycloidal speed reducer are written as:

$$\begin{cases} I_a\ddot{\theta}_a + c_a(\dot{\theta}_a - \dot{\theta}_l) + k_a(\theta_a - \theta_l) = T_a \\ I_l\ddot{\theta}_l + 2c_h a^2(\dot{\theta}_l - \dot{\theta}_l') + 2k_h a^2(\theta_l - \theta_l') = c_a(\dot{\theta}_a - \dot{\theta}_l) + k_a(\theta_a - \theta_l) \\ I_{mi}\ddot{\theta}_{mi} + hc_q(\dot{\theta}_{mi} - \dot{\theta}_o){R_o}^2 + hk_q(\theta_{mi} - \theta_o){R_o}^2 = \\ \sum_{j=1}^{n} c_{mj}L_{mj}^2(\dot{\theta}_{li}'i_m - \dot{\theta}_{mi} - \dot{e}_j/L_{mj}) + \sum_{j=1}^{n} k_{mj}L_{mj}^2(\theta_{li}'i_m - \theta_{mi} - e_{2kj}/L_{mj}) \\ I_o\ddot{\theta}_o + T_o = hc_q{R_o}^2(\dot{\theta}_{m1} + \dot{\theta}_{m2} - 2\dot{\theta}_o) + hk_q{R_o}^2(\theta_{m1} + \theta_{m2} - 2\theta_o) \\ i = 1, 2 \end{cases} \tag{15}$$

where $\theta_l - \theta_l'$ is the relative displacement of cycloid disc and crank shaft. Subscript i is represents the i-th cycloid disc. Subscript j is represents the j-th cycloid disc meshing tooth pair. n is the total number of cycloid disc meshing tooth pair. h is the total number of output rollers.

L is shown in Fig. 1(B).

e is the amplitude of cycloid disc teeth profile error. In this example, e is the modification clearance.

4.1. Mesh stiffness calculation

Cycloid disc teeth is taking as a non-uniform cantilever beam in this paper.

The bending, shear and axial compressive energy stored in a tooth can be represented by [24,25] as follows

$$U_b = \frac{F^2}{2K_b},\ U_s = \frac{F^2}{2K_s},\ U_c = \frac{F^2}{2K_c} \tag{16}$$

where K_b, K_s, K_c are the bending, shear and axial compressive stiffness respectively.

The potential energy stored in the bending, shear and axial compressive deformations can be expressed as

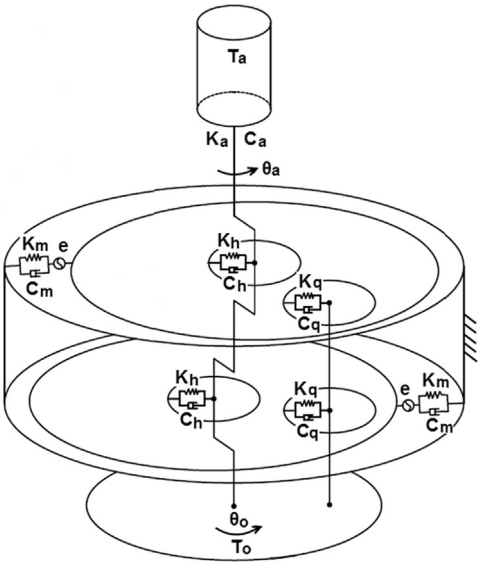

Fig. 10. Dynamic model of cycloidal speed reducer.

$$U_b = \int_0^d \frac{M^2}{2EI_x}dx,\ U_s = \frac{F^2}{2K_s} = \int_0^d \frac{1.2F_s^2}{2GA_x}dx,\ U_c = \frac{F^2}{2K_c} = \int_0^d \frac{F_a^2}{2EA_x}dx \tag{17}$$

where $F$is the mesh force. And F_b, F_a and M are calculated by

$$F_b = F\cos\alpha \tag{18}$$

$$F_a = F\sin\alpha \tag{19}$$

$$M = F_b{\cdot}x - F_a{\cdot}h \tag{20}$$

Based on Eqs. (16)–(20), the bending, shear and axial compressive stiffness can be obtained as,

$$\frac{1}{K_b} = \int_0^d \frac{(x\cos\alpha - h\sin\alpha)^2}{EI_x}dx \tag{21}$$

$$\frac{1}{K_s} = \int_0^d \frac{1.2\cos^2\alpha}{GA_x}dx \tag{22}$$

$$\frac{1}{K_c} = \int_0^d \frac{\sin^2\alpha}{EA_x}dx \tag{23}$$

In the formulas (17)–(23), h, x, dx, α, d are shown in Fig. 11. E is the elasticity modulus. G represents the shear modulus. I_x and A_x represent the area moment of inertia and area of the section where the distance between the section and the acting point of the applied force is x, and they can be expressed as

$$I_x = \frac{2}{3}h_x^3 W \tag{24}$$

$$A_x = 2h_x W \tag{25}$$

$$G = \frac{E}{2(1+\mu)} \tag{26}$$

where μ is the Poisson ratio. h_x is the distance between a point and the tooth's central line and this point lies on the tooth profile curve where the vertical distance from the tooth's root is equal to d minus x..

The Hertzian contact stiffness K_h is given by [26] as follows

$$K_h = \frac{\pi EW}{4(1-\mu^2)} \tag{27}$$

Ignore the bending, shear and axial compressive stiffness of pins, the total equivalent mesh stiffness of one tooth pair of cycloid disc in mesh can be expressed as:

$$K_m = \frac{1}{\frac{1}{K_b} + \frac{1}{K_s} + \frac{1}{K_a} + \frac{1}{K_h}} \tag{28}$$

The cycloid disc mesh stiffness is calculated according to Eq. (28) and is shown in Fig. 12.

4.2. Simulation and discussion of cycloidal speed reducer system

In order to compare the simulation results of different cycloid disc teeth profile modification, there are two modification targets adopted in this simulation, which are the contact stress and the contact force. The mesh stiffness calculated by the mathematical model in Section 3.1 is plugged into the dynamic Eq. (15), other parameters are shown in Table 2. Then the cycloid disc rotational displacement and rotational velocity versus time can be obtained through solving the equation using the Runge-kutta numerical

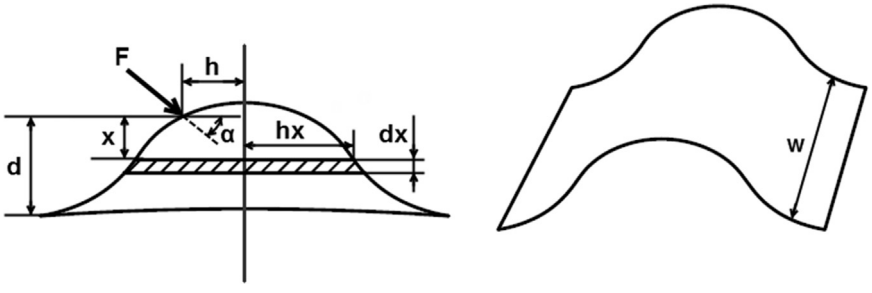

Fig. 11. Mode of the cycloid disc tooth as a non-uniform cantilever beam.

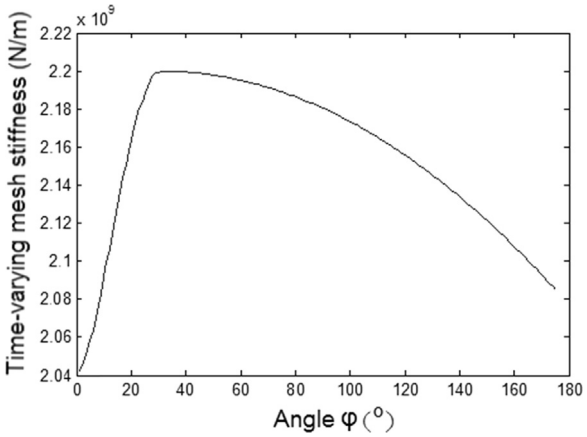

Fig. 12. Time-varying mesh stiffness of singe tooth of cycloid disc.

Table 2
Parameters of the cycloidal speed reducer dynamic model.

parameters	value
Moment of inertia of crank shaft (kg m^2)	0.0022
Moment of inertia of cycloid disc (kg m^2)	0.04
Moment of inertia of output shaft (kg m^2)	0.13
Damping between meshing teeth of cycloid disc (Ns/m)	1.0×10^3
Damping of the bearing (Ns/m)	1.8×10^3
Damping of the output rollers (Ns/m)	4.0×10^4
Stiffness of the output rollers (N/m)	4.4×10^6
Stiffness of the bearing (N/m)	6.56×10^7

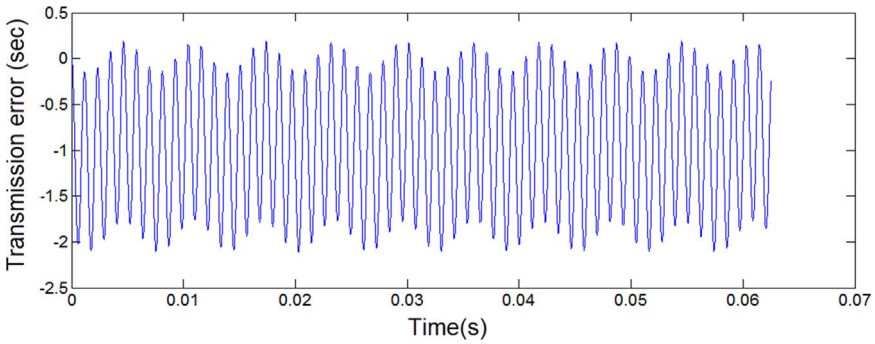

Fig. 13. The rotational displacement fluctuation deviation of cycloid disc when. the cycloid disc teeth profile modification target is contact stress.

method. The result of the cycloid disc rotational displacement is presented in Fig. 13 where the modification target is contact stress. The result for contact force is shown in Fig. 14.

As shown in Figs. 13 and 14, cycloid disc teeth profile modification clearance will cause the difference of the vibration amplitude when the modification clearance changes. For the case of the contact stress, the rotational displacement fluctuation deviation of cycloid disc is nearly 2 s. The rotational displacement fluctuation deviation of cycloid disc is nearly 3 s when the cycloid disc teeth profile modification target is contact stress.

The results show that optimize the cycloid disc tooth modification curve can improve the carrying capability of cycloidal speed reducer, eliminate noise and vibration and develop the transmission accuracy.

5. Conclusion

A new tooth profile modification method presented was proposed in this paper. A new clearance curve which could be defined by adjusting the position of 5 key points was developed in this method. It allows us to define the position of minimum clearance and the modification on the heel and toe end of cycloid disc teeth, which is more flexible compared with current cycloid disc tooth

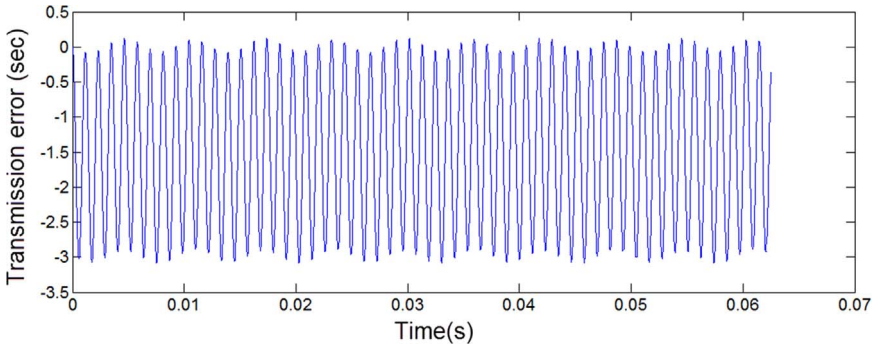

Fig. 14. The rotational displacement fluctuation deviation of cycloid disc when. the cycloid disc teeth profile modification target is contact force.

modification method. We also establish a dynamic mathematic model of cycloidal speed reducer system. With the comparison of two numerical experiments and dynamic simulation, the results indicate that the new method can improve the carrying capability of cycloidal speed reducer, develop the transmission accuracy, and deduce the vibration and noise of cycloidal speed reducer.

Acknowledgments

This project is supported by National Natural Science Foundation of China (Grant Nos. 51405250 and 51475354).

References

[1] D.W. Botsiber, L. Kingston, Cycloid speed reducer, Mach. Des. (1956) 65–69.
[2] E.P. Pollitt, Some applications of the cycloid in machine design, ASME J. Eng. Ind. (1960) 407–414.
[3] V.N. Kudrijavcev, Planetary gear train (in Russian), Mech. Eng. (1966).
[4 M. Lehmann, Calculation and Measurement of Forces Acting on Cycloid Speed Reducer (in German) (Ph.D. Thesis), Technical University Munich, Germany, 1976.
[5] S.K. Malhotra, M.A. Parameswaran, Analysis of a cycloid speed reducer, Mech. Mach. Theory 18 (6) (1983) 491–499.
[6] F. Litvin, P. Feng, Computerized design and generation of cycloidal gearings, Mech. Mach. Theory 31 (7) (1996) 891–911.
[7] C.F. Hsieh, Study on Geometry Design of Rotors Using Trochoidal Curve (Ph.D. Dissertation), Department of Mechanical Engineering, National Chung Cheng University, Taiwan, 2006.
[8] J.W. Sensinger, Unified approach to cycloid drive profile, stress, and efficiency optimization, ASME J. Mech. Des. 132 (2010) 024503-1(~5).
[9] J.G. Blanche, D.C.H. Yang, Cycloid drives with machining tolerances, J. Mech. Trans. Autom. Des. 111 (1989) 337–344.
[10] D.C.H. Yang, J.G. Blanche, Design and application guidelines for cycloid drives with machining tolerances, Mech. Mach. Theory 25 (5) (1990) 487–501.
[11] W. Yongkuan, Z. Jianyun, C. Tianqi, L. Lixing, The analysis research of the geometric lost motion of high accurate RV reducer used in robot, J. Dalian Inst. Railw. Technol. 20 (2) (1999) 24–27.
[12] C.S. Huang, On the Surface Design, Tooth Contact Analysis, and Optimum Design of Cycloidal Drives with Modified Tooth Profiles (M.S. Thesis), Department of Mechanical Engineering, National Cheng Kung University, Taiwan, 2006.
[13] M. Chmurawa, A. Lokiec, Distribution of loads in cycloidal planetary gear (CYCLO) including modification of equidistant, in: Proceedings of the 16th European ADAMS User Conference, Berchtesgaden, Germany, 2001.
[14] M. Chmurawa, A. John, Numerical analysis of forces,stress and strain in planetary wheel of cycloidal gear using FEM, Numer. Methods Contin. Mech. Liptovsky Jan. Slovak Repub. (2000).
[15] M. Yunhong, W. Changlin, L. Liping, Mathematical modeling of the transmission performance of 2K-H pin cycloid planetary Mechanism, Mech. Mach. Theory 42 (7) (2007) 776–790.
[16] Y.-W. Hwang, C.-F. Hsieh, Geometric design using hypotrochoid and nonundercutting conditions for an internal cycloidal gear, ASME J. Mech. Des. 129 (2007) 413–420.
[17] M. Blagojevic´, Stress and Strain State of Cyclo Speed Reducer's Elements Under Dynamic Loads (in Serbian) (Ph.D. Thesis), Faculty of Mechanical Engineering, Kragujevac, Serbia, 2008.
[18] M. Blagojevic´, V. Nikolic´, N. Marjanovic´, L.J. Veljovic´, Analysis of cycloid drive dynamic behavior, Sci. Tech. Rev. LIX (1) (2009) 52–56.
[19] A. Kahraman, H. Ligata, A. Singh, Influence of ring gear rim thickness on planetary gear set behavior, J. Mech. Des. 132 (2) (2010) 021002.
[20] G. Haijun, Accuracy of Analysis and Simulation Study of the 2K-V Type Cycloid Drive, Northwestern Polytechnic University.
[21] H. Linshan, S. Yunwen, D. Haijun, Research on dynamic transmission accuracy for 2K-V-type drive, Chin. J. Mech. Eng. 43 (6) (2007) 81–86.
[22] Editorial Board of Machinerys Handbook, Machinerys Handbook (Gear Train), China Machine Press, Beijing, 2007.
[23] Wan-Sung Lin, Design of a two-stage cycloidal gear reducer with tooth modifications, Mech. Mach. Theory 79 (2014) 184–197.
[24] D.C.H. Yang, Lin J.Y. Hertzian Damping, Tooth friction and bending elasticity in gear impact dynamics, J. Mech. Transm. AUT Des. 109 (2) (1987) 189–196.
[25] X.H. Tian, Dynamic Simulation for System Response of Gearbox Including Localized Gear Faults (Master's Thesis), University of Alberta, Edmonton, Alberta, Canada, 2004.
[26] D.C.H. Yang, Z.S. Su, A rotary model for spur gear dynamics, ASME J. Mech. Trans. AUT Des. 107 (1985) 529–535.